Role of the *XIST-miR-181a-COL4A1* axis in the development and progression of keratoconus

Rui Tian, Lufei Wang, He Zou, Meijiao Song, Lu Liu, Hui Zhang

Department of Ophthalmology, the Second Hospital of Jilin University, Changchun 130000, Jilin Province, China

Background: As a disorder occurs in the eyes, keratoconus (KC) is induced by the thinning of the corneal stroma. This study was designed to reveal the key long non-coding RNAs (lncRNAs), microRNAs (miRNAs), and mRNAs involved in the mechanisms of KC.

Methods: Transcriptome RNA-seq data set GSE112155 was acquired from the Gene Expression Omnibus database, which contained 10 KC samples and 10 myopic control samples. Using the edgeR package, the differentially expressed (DE)-mRNAs between KC and control samples were screened. The DE-lncRNAs and DE-miRNAs in this data set were identified using the HUGO Gene Nomenclature Committee (HGNC). Using the pheatmap package, bidirectional hierarchical clustering of the DE-RNAs was conducted. Then, an enrichment analysis of the DE-mRNAs was performed using the DAVID tool. Moreover, a competitive endogenous RNA (ceRNA) regulatory network was built using the Cytoscape software. After KC-associated pathways were searched within the Comparative Toxicogenomics Database, a KC-associated ceRNA regulatory network was constructed.

Results: There were 282 DE-lncRNAs (192 upregulated and 90 downregulated), 40 DE-miRNAs (29 upregulated and 11 downregulated), and 910 DE-mRNAs (554 upregulated and 356 downregulated) between the KC and control samples. A total of 34 functional terms and 9 pathways were enriched for the DE-mRNAs. In addition, 6 mRNAs (including *PPARG*, *HLA-B*, *COL4A1*, and *COL4A2*), 5 miRNAs (including *miR-181a*), 9 lncRNAs (including *XIST*), and the *XIST-miR-181a-COL4A1* axis were involved in the KC-associated ceRNA regulatory network.

Conclusions: *PPARG*, *HLA-B*, *COL4A1*, *COL4A2*, *miR-181a*, and *XIST* might be correlated with the development of KC. Further, the *XIST-miR-181a-COL4A1* axis might be implicated in the pathogenesis of KC.

As a disease of the eye, keratoconus (KC) leads to the uninflammatory thinning of the corneal stroma [1]. KC usually occurs in the transition period from childhood to adulthood, and it is more common in Asian populations [2]. KC may induce the symptoms of double vision, nearsightedness, blurry vision, light sensitivity, and astigmatism [3]. KC patients may need special contact lenses or even corneal transplantation [4,5].

KC is caused by genetic, hormonal, and environmental factors [6], and genetic and environmental factors contribute to the pathogenesis and development of KC. Previous studies have shown that the alteration of inflammatory factors and genetic molecules is associated with KC [7-9]. For instance, Pahuja et al. [8] and Shetty et al. [10] showed that the levels of inflammatory factors such as tumor-necrosis factor (TNF)-α, interleukin (IL)-6, and matrix metalloproteinase 9 (MMP-9) were elevated in the epithelium of KC patients. Long non-coding RNA (lncRNA), microRNAs (miRNAs), and several pathways—including transforming growth factor β (TGF-β),

phosphatidylinositol 3-kinase (PI3K)/protein kinase B (Akt), and Wnt signaling pathways—may function in the development and progression of KC [7,9,11]. The expression of *miR-184* in normal cornea samples is higher than that of *miR-205*, and *miR-184* may act in cornea development and corneal diseases [12,13]. Calpastatin plays a role in genetic susceptibility to KC, and the differential modulation of calpain–calpastatin complex may influence the functional defect of the cornea [14]. Downregulated β-actin may be correlated with decreased human antigen R (HuR) in the corneal stroma of KC patients, which may also serve as a risk factor for the occurrence and development of KC [15]. However, the key RNAs involved in the pathogenesis of KC have not been comprehensively identified, and the pathogenesis of KC remains unclear.

In recent years, more and more evidence has shown that the mutual regulation models between lncRNA and miRNA and their downstream target genes are closely related to the occurrence and development of diseases [16,17]. As an important factor in post-transcriptional regulation, miRNA activity can be regulated by lncRNA through sponge adsorption [18]. As competitive endogenous RNA (ceRNA), lncRNA competitively binds to miRNA to regulate the protein level of the coding gene and participates in the regulation of cell

Correspondence to: Hui Zhang, Department of Ophthalmology, the Second Hospital of Jilin University, No. 218 Ziqiang Street, Nan Guan District, Changchun 130000, Jilin Province, China; Phone: +86-0430-81136545; FAX: +86-0430-81136545; email: zhanghui_m04@163.com
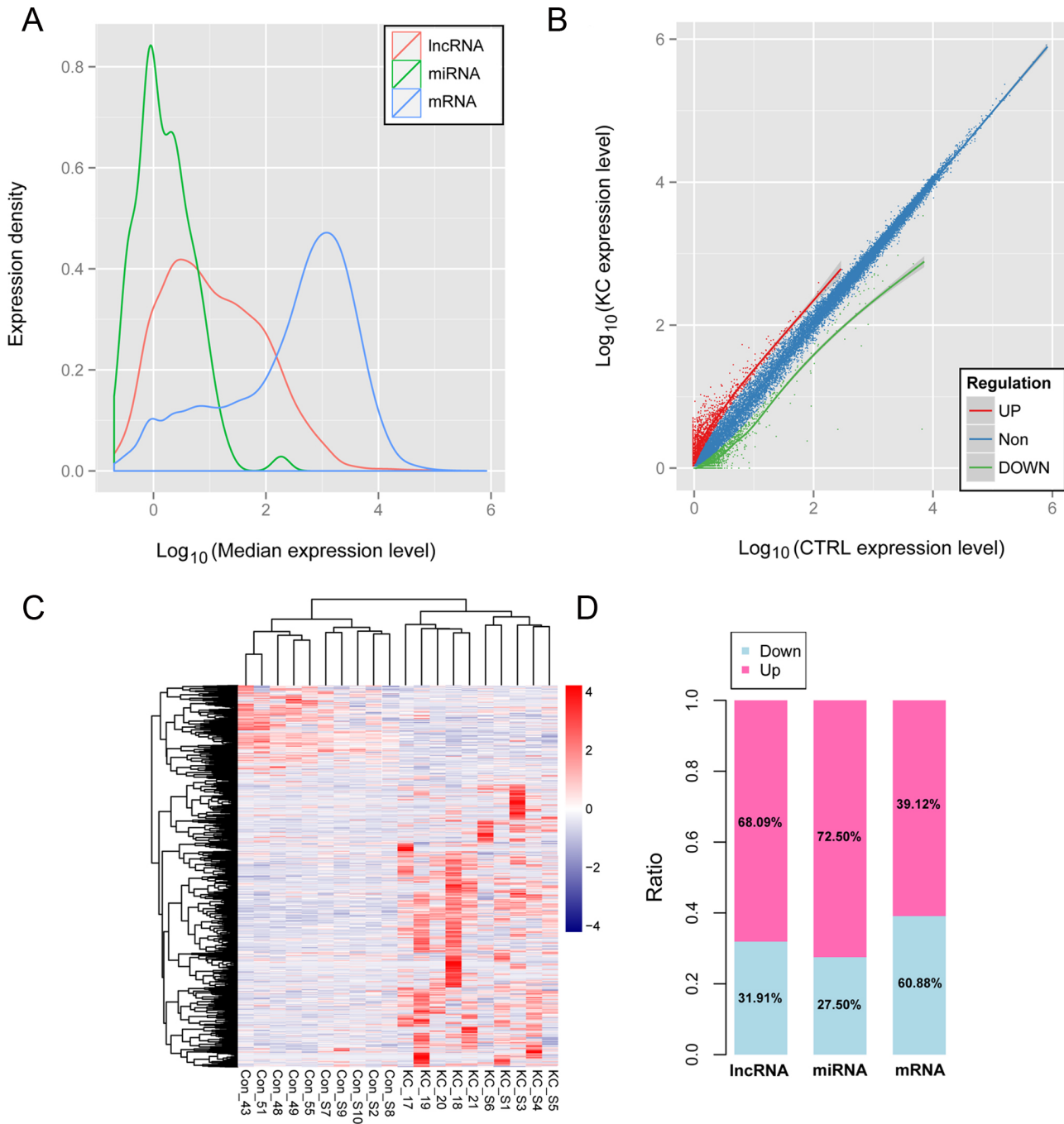
Figure 1. The expression distribution curves, scatter diagram, clustering heatmap, and histogram of the differentially expressed RNAs (DE-RNAs). **A**: The expression distribution curves of the identified RNAs. The red, green, and blue curves represent long non-coding RNAs (lncRNAs), microRNAs (miRNAs), and mRNAs, respectively. **B**: The scatter diagram of the DE-RNAs. The red, green, and blue dots represent significantly upregulated RNAs, significantly downregulated RNAs, and non–DE-RNAs, respectively. **C**: The clustering heatmap of the DE-RNAs. **B**: The histogram showing the proportion of upregulated and downregulated RNAs.

biologic behaviors [19]. Therefore, in-depth research into the control mechanism of ceRNA will help us better understand the occurrence and development of diseases.

By analyzing the gene expression profile of KC, the differentially expressed (DE)-RNAs between KC samples and myopic control samples were screened. Following this, a ceRNA regulatory network was built to select the key RNAs

TABLE 1. THE RESULTS OF ENRICHMENT ANALYSIS FOR THE DIFFERENTIALLY EXPRESSED mRNAs.

Category	Term	Count	P-value	FDR
Biology Process	GO:0006811~ion transport	78	1.69E-11	3.01E-08
	GO:0007267~cell-cell signaling	62	1.49E-09	2.65E-06
	GO:0009611~response to wounding	55	1.30E-08	2.31E-05
	GO:0030001~metal ion transport	49	5.78E-08	1.03E-04
	GO:0006955~immune response	63	1.17E-07	2.08E-04
	GO:0006812~cation transport	54	1.34E-07	2.40E-04
	GO:0002526~acute inflammatory response	19	3.03E-07	5.39E-04
	GO:0006952~defense response	57	3.18E-07	5.67E-04
	GO:0006959~humoral immune response	17	3.43E-07	6.11E-04
	GO:0019226~transmission of nerve impulse	39	4.14E-07	7.37E-04
	GO:0007268~synaptic transmission	35	5.40E-07	9.62E-04
	GO:0006954~inflammatory response	36	1.44E-06	2.56E-03
	GO:0006956~complement activation	12	1.63E-06	2.90E-03
Cellular Component	GO:0005576~extracellular region	166	8.85E-13	1.22E-09
	GO:0005886~plasma membrane	264	2.56E-12	3.53E-09
	GO:0044421~extracellular region part	97	4.47E-12	6.16E-09
	GO:0044459~plasma membrane part	173	1.84E-11	2.54E-08
	GO:0031224~intrinsic to membrane	348	1.92E-11	2.65E-08
	GO:0005615~extracellular space	74	1.32E-10	1.83E-07
	GO:0016021~integral to membrane	334	2.43E-10	3.35E-07
	GO:0031226~intrinsic to plasma membrane	106	2.24E-09	3.10E-06
	GO:0005887~integral to plasma membrane	104	2.84E-09	3.92E-06
	GO:0034702~ion channel complex	27	6.91E-06	0.009529
Molecular Function	GO:0015267~channel activity	51	1.14E-10	1.74E-07
	GO:0005216~ion channel activity	49	1.17E-10	1.78E-07
	GO:0022803~passive transmembrane transporter activity	51	1.24E-10	1.88E-07
	GO:0022838~substrate specific channel activity	49	3.38E-10	5.15E-07
	GO:0022836~gated channel activity	40	4.97E-09	7.56E-06
	GO:0005261~cation channel activity	33	7.27E-07	1.11E-03
	GO:0005509~calcium ion binding	71	7.41E-06	1.13E-02
	GO:0046873~metal ion transmembrane transporter activity	34	1.19E-05	1.81E-02
	GO:0022834~ligand-gated channel activity	19	1.40E-05	2.13E-02
	GO:0015276~ligand-gated ion channel activity	19	1.40E-05	2.13E-02

| Category	Term	Count	P-value	FDR
	GO:0030594~neurotransmitter receptor activity	16	1.97E-05	2.99E-02
Pathway	hsa04080:Neuroactive ligand-receptor interaction	35	7.65E-08	1.07E-05
	hsa04610:Complement and coagulation cascades	15	5.01E-06	3.51E-04
	hsa04940:Type I diabetes mellitus	11	2.69E-05	1.26E-03
	hsa00982:Drug metabolism	13	3.97E-05	1.39E-03
	hsa00140:Steroid hormone biosynthesis	10	3.43E-04	9.55E-03
	hsa04060:Cytokine-cytokine receptor interaction	26	1.07E-03	2.47E-02
	hsa05330:Allograft rejection	8	1.64E-03	3.22E-02
	hsa04020:Calcium signaling pathway	19	2.53E-03	3.86E-02
	hsa00980:Metabolism of xenobiotics by cytochrome P450	10	2.51E-03	4.30E-02

Note: FDR, false discovery rate.
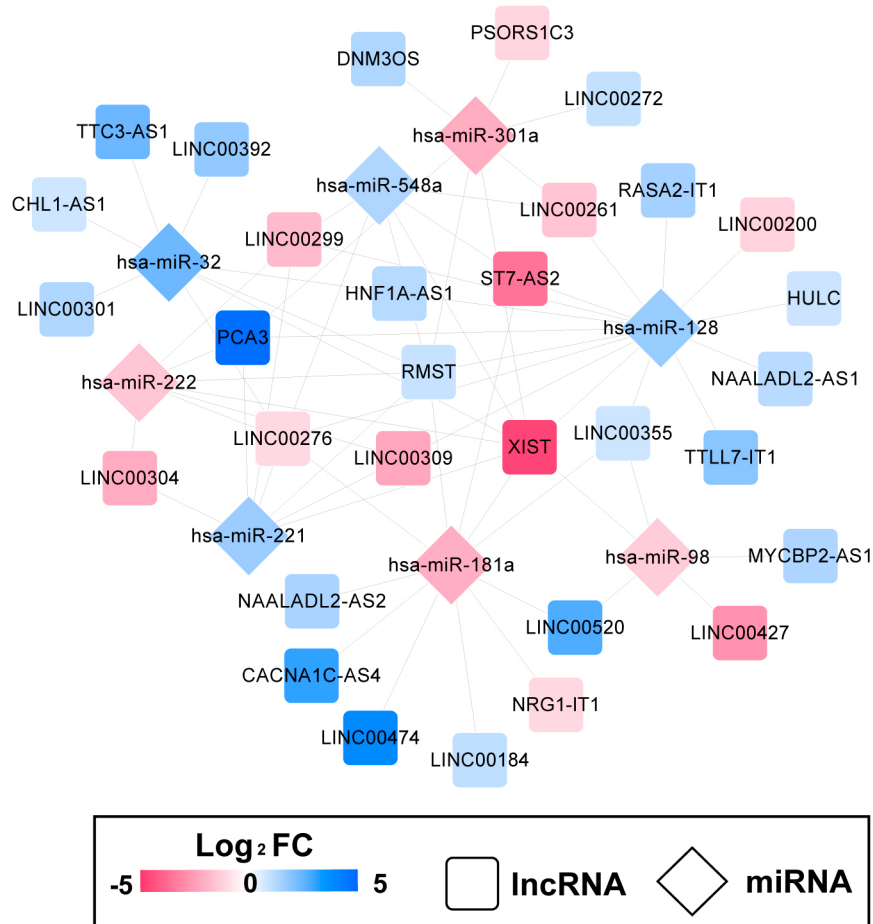
Figure 2. The long non-coding RNA (lncRNA)–microRNA (miRNA) regulatory network. The squares and diamonds represent lncRNAs and miRNAs, respectively. Blue and red represent upregulation and downregulation, respectively.

affecting the development of KC from those in myopia. This study might help to reveal the ceRNA regulatory mechanisms correlated with the pathogenesis of KC.

METHODS

Data preprocessing and differential expression analysis: Transcriptome RNA-seq data set GSE112155 was downloaded from the Gene Expression Omnibus (GEO) database. There were 20 cornea epithelial tissue samples in GSE112155, including 10 KC samples (10 males) and 10 myopic control samples (6 males and 4 females). Female control samples were included in our study to avoid a gender bias, as reported by You [20]. The expression profile data related to read count level was normalized using R package preprocessCore (version 1.40.0, Berkeley, CA) [21].

The lncRNAs, miRNAs, and mRNAs in GSE112155 were annotated and identified in the HUGO Gene Nomenclature Committee (HGNC) database [22], which includes 3,979 lncRNAs, 1,932 miRNAs and 19,197 recognized protein-coding genes. Using R package edgeR (version 3.22.5) [23], the DE-lncRNAs, DE-miRNAs, and DE-mRNAs between the KC and control samples were analyzed. A |log2 fold change (FC)| of >1 and false discovery rate (FDR) of <0.05 were selected as the thresholds of significant differential expression.

Hierarchical clustering analysis and enrichment analysis: For the screened DE-RNAs, bidirectional hierarchical clustering based on a correlation algorithm was performed using the R package pheatmap (version 1.0.8) [24]. In addition, using the DAVID tool (version 6.8, Frederick, MD) [25], the DE-mRNAs were analyzed though the Gene Ontology (GO) enrichment analysis, which included the Biology Process (BP), Molecular Function (MF), and Cellular Component (CC) categories [26], and through the Kyoto Encyclopedia of Genes and Genomes (KEGG) enrichment analysis [27].

A p value of <0.05 was taken as the threshold of enrichment significance.

Regulatory network analysis of ceRNA: As a kind of ceRNA within miRNA, lncRNA is involved in the expression regulation of target genes and plays an important role in the occurrence and development of diseases [28]. The lncRNA–miRNA regulatory pairs in the miRecode (version 11, Gothenburg, Sweden) [29] and starBase (version 2.0, Guangzhou, China) [30] databases were merged, and the regulatory pairs between DE-lncRNAs and DE-miRNAs were then screened from them. Using the Cytoscape software (version 3.6.1, Bethesda, MD) [31], the lncRNA–miRNA regulatory network was visualized.

Using the starBase database [30], the target genes were predicted for the DE-miRNAs involved in the identified lncRNA–miRNA pairs. The starBase database integrates target prediction information from the targetScan, picTar, RNA22, PITA, and miRanda databases [30]. In this study, miRNA-target regulatory pairs included in at least one of the five databases were selected. Subsequently, the DE-mRNAs were correlated with the predicted target genes, and only the

miRNA-target regulatory pairs involved the DE-miRNAs and DE-mRNAs with opposite expression change directions were retained. Moreover, the miRNA–mRNA regulatory network was built using the Cytoscape software [31].

Along with the identified lncRNA–miRNA and miRNA–mRNA regulatory pairs, the ceRNA regulatory network was constructed using the Cytoscape software [31]. In addition, DAVID tool [25] was used to enrich the KEGG pathways for the mRNAs implicated in the ceRNA regulatory network, with a p value of <0.05 as the significance threshold.

Construction of KC-associated ceRNA regulatory network: Using "keratoconus" as the keyword, the KEGG pathways directly correlated with KC were searched in the Comparative Toxicogenomics Database (Raleigh, NC) [32]. To obtain the mRNAs participating in the KC-associated pathways, the searched pathways were compared with the pathways enriched for the mRNAs implicated in the ceRNA regulatory network. Finally, the regulatory pairs involving the mRNAs enriched in the KC-associated pathways were extracted from the ceRNA regulatory network to construct the KC-associated ceRNA regulatory network.

Figure 3. The microRNA (miRNA)–mRNA regulatory network. The diamonds and circles represent miRNAs and mRNAs, respectively. Blue and red represent upregulation and downregulation, respectively.

TABLE 2. THE PATHWAYS ENRICHED FOR THE MRNAS IMPLICATED IN THE COMPETING
ENDOGENOUS RNA (CERNA) REGULATORY NETWORK.

Term	Count	P-value	Genes
hsa04510:Focal adhesion	5	0.001561	*COL4A2, COL4A1, CCND2, TNC, KDR*
hsa04060:Cytokine-cytokine receptor interaction	5	0.003707	*CXCL1, CCL22, CXCL5, KDR, CXCL10*
hsa04062:Chemokine signaling pathway	4	0.006217	*CXCL1, CCL22, CXCL5, CXCL10*
hsa04512:ECM-receptor interaction	3	0.006331	*COL4A2, COL4A1, TNC*
*hsa04940:Type I diabetes mellitus	2	0.018766	*CPE, HLA-B*
*hsa05200:Pathways in cancer	4	0.021608	*COL4A2, COL4A1, PPARG, RUNX1T1*
hsa04623:Cytosolic DNA-sensing pathway	2	0.023854	*IL33, CXCL10*
hsa04270:Vascular smooth muscle contraction	2	0.042772	*EDNRA, PRKG1*

Note: "*" indicates the pathways overlapped with the keratoconus-correlated pathways searched from Comparative Toxicogenomics Database.

RESULTS

Data preprocessing and differential expression analysis:
A total of 22,281 RNAs were detected in transcriptome RNA-seq data set GSE112155. Based on the HGNC database, 3,261 lncRNAs, 789 miRNAs, and 18,231 mRNAs were

identified. The expression distribution curves of the identified lncRNAs, miRNAs, and mRNAs are shown in Figure 1A. There were 282 DE-lncRNAs (192 upregulated and 90 downregulated), 40 DE-miRNAs (29 upregulated and 11 downregulated), and 910 DE-mRNAs (554 upregulated and
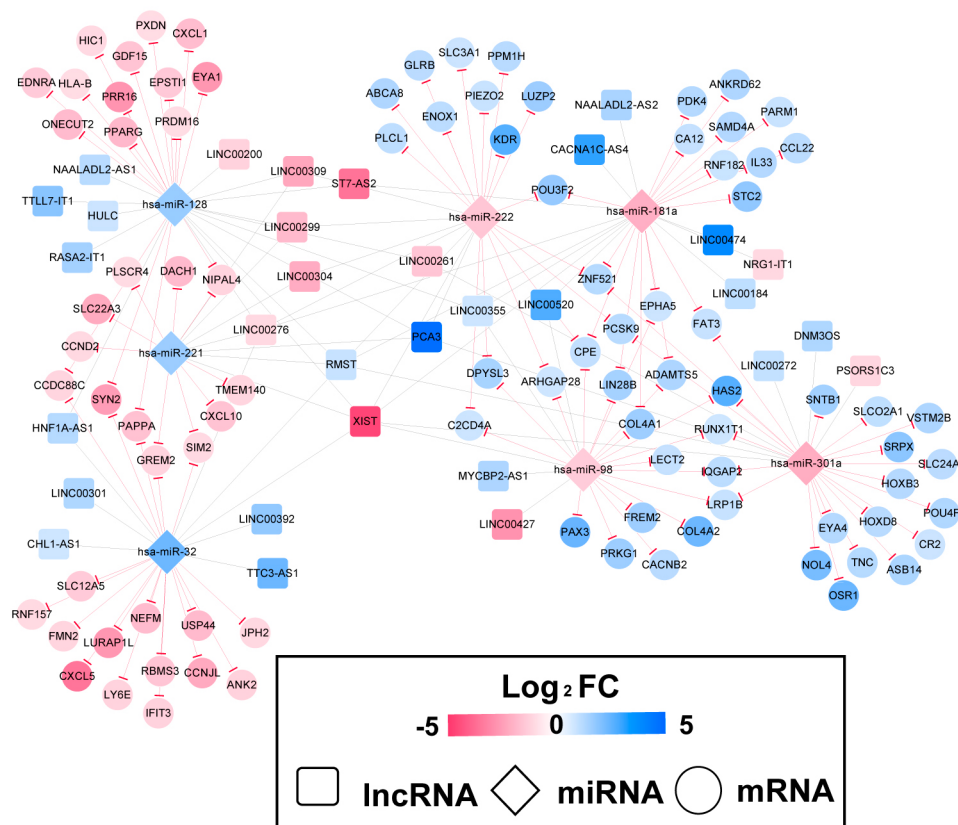

Figure 4. The competing endogenous RNA (ceRNA) regulatory network. The squares, diamonds, and circles represent long non-coding RNAs (lncRNAs), microRNAs (miRNAs), and mRNAs, respectively. Blue and red represent upregulation and downregulation, respectively. Black lines and red lines represent, respectively, lncRNA–miRNA and miRNA–mRNA relationships.

356 downregulated) between the KC and control samples. A scatter diagram of the screened DE-RNAs is presented in Figure 1B.

Hierarchical clustering analysis and enrichment analysis: A clustering heatmap showed that the expression values of the screened DE-RNAs could separate different types of samples (Figure 1C,D). The result suggested that the DE-RNAs had expression characteristics in the samples. Enrichment analysis showed that 13 GO_BP terms (such as ion transport), 10 GO_CC terms (such as extracellular region), 11 GO_MF terms (such as channel activity), and 9 KEGG pathways (such as neuroactive ligand-receptor interaction) were enriched for the DE-mRNAs (Table 1).

Analysis of the ceRNA regulatory network: After 66 eligible lncRNA–miRNA pairs were obtained, the lncRNA–miRNA regulatory network (involving 31 lncRNAs and 8 miRNAs) was built (Figure 2). Afterwards, 116 miRNA–mRNA

regulatory pairs were acquired to construct the miRNA–mRNA regulatory network (involving 7 miRNAs and 92 mRNAs; Figure 3).

Then, lncRNA–miRNA–mRNA regulatory pairs were then identified, and the ceRNA regulatory network was constructed (Figure 4). In the ceRNA regulatory network, there were 131 nodes (including 32 lncRNAs, 7 miRNAs, and 92 mRNAs) and 182 edges (including 66 lncRNA–miRNA pairs and 116 miRNA–mRNA pairs). Additionally, 8 KEGG pathways (such as focal adhesion) were enriched for the mRNAs implicated in the ceRNA regulatory network (Table 2).

Construction of KC-associated ceRNA regulatory network: Only 12 KEGG pathways directly correlated with KC were found in the Comparative Toxicogenomics Database. After comparing the searched pathways with the pathways enriched for the mRNAs implicated in the ceRNA regulatory network,
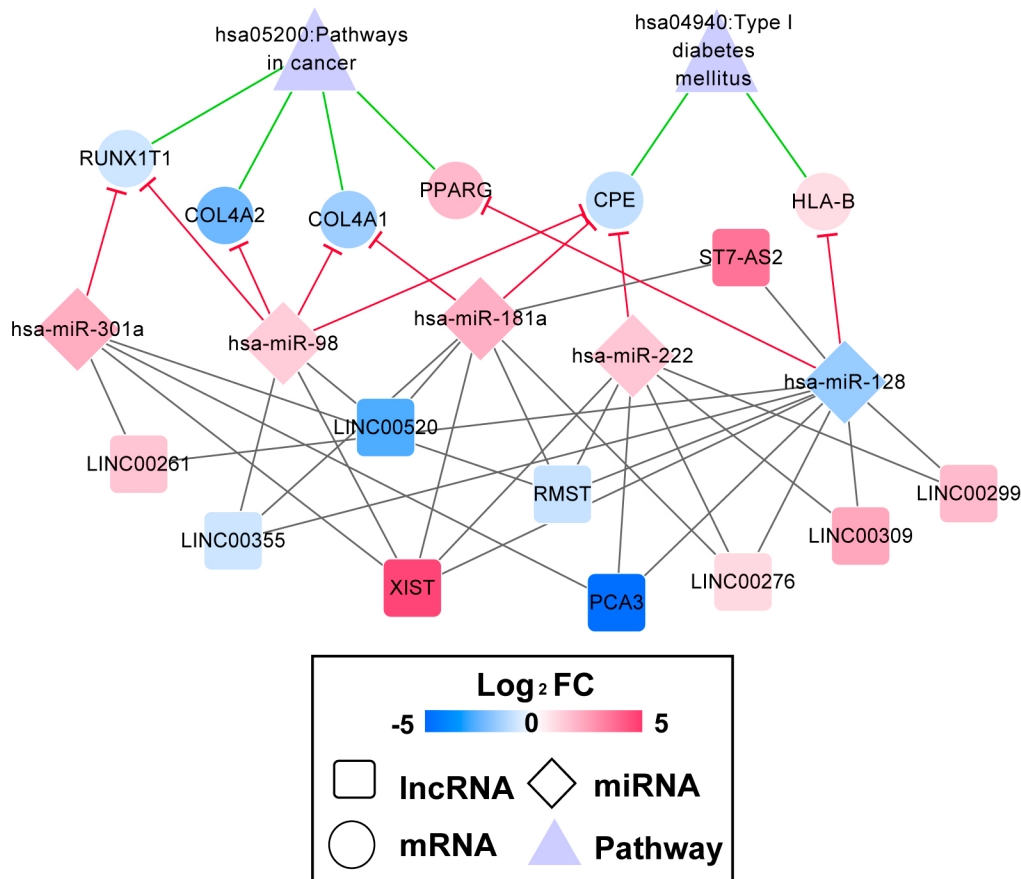

Figure 5. The keratoconus (KC)-associated competing endogenous RNA (ceRNA) regulatory network. The squares, diamonds, and circles represent long non-coding RNAs (lncRNAs), miRNAs, and mRNAs, respectively. Blue and red represent upregulation and downregulation, respectively. Black lines and red lines represent, respectively, lncRNA–miRNA and miRNA–mRNA relationships. Purple triangles represent KC-associated pathways.
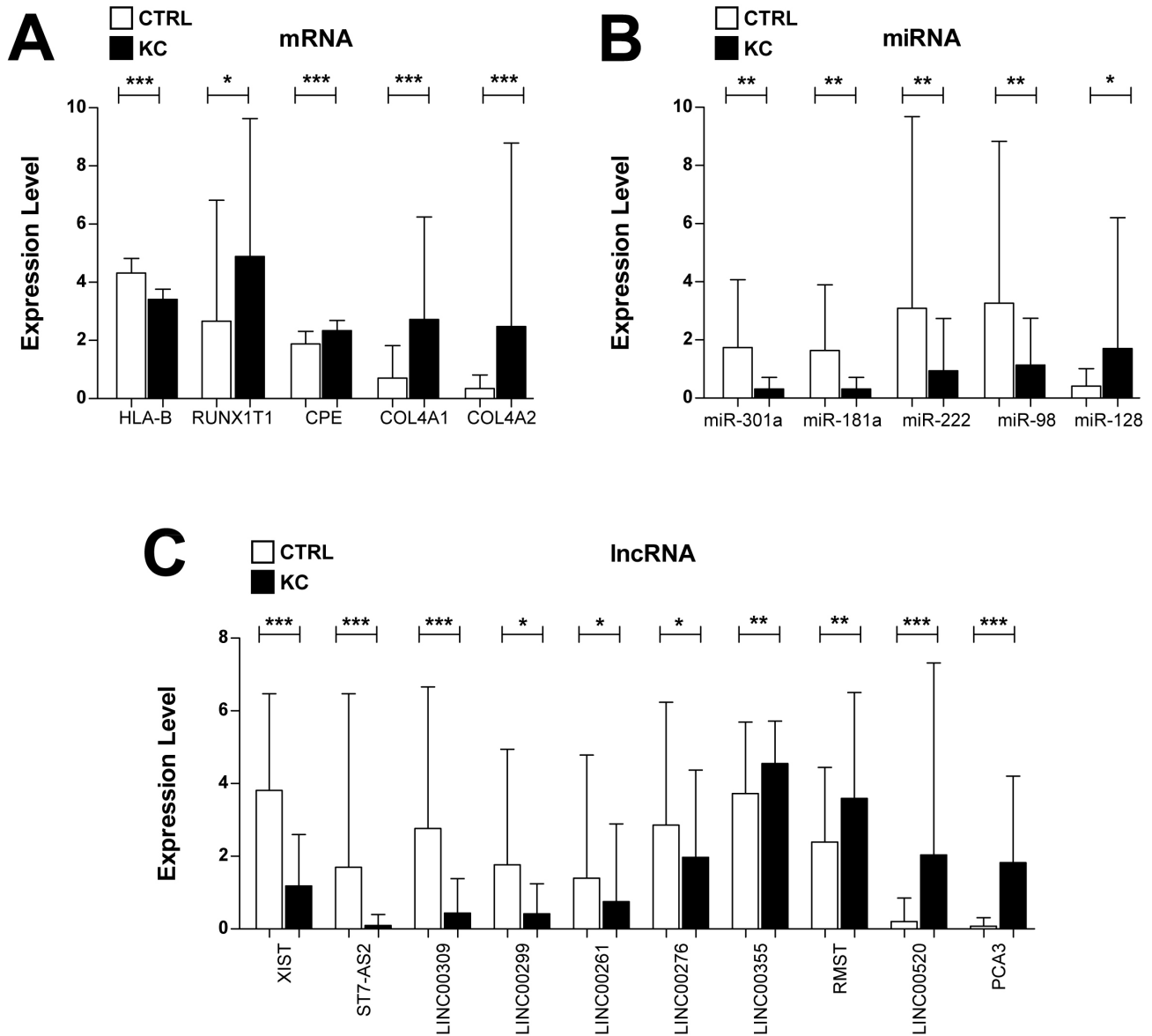
Figure 6. The expression levels of the RNAs correlated with keratoconus (KC). **A:** The expression levels of the mRNAs correlated with KC. **B:** The expression levels of the microRNAs (miRNAs) correlated with KC. **C:** The expression levels of the long non-coding RNAs (lncRNAs) correlated with KC. Black and white columns represent KC samples and control samples, respectively.

two overlapping pathways (type I diabetes mellitus, and pathways in cancer) were obtained as KC-associated pathways. Subsequently, the KC-associated ceRNA regulatory network was built (Figure 5). Meanwhile, the RNAs correlated with KC were obtained, including 6 mRNAs (peroxisome proliferator-activated receptor gamma [*PPARG*]; human leukocyte antigen-B [*HLA-B*]; runt-related transcription factor 1 [*RUNX1T1*]; carboxypeptidase E [*CPE*]; collagen, type IV, alpha 1 [*COL4A1*]; and collagen, type IV, alpha 2 [*COL4A2*]),

5 miRNAs (*miR-301a*, *miR-181a*, *miR-222*, *miR-98*, and *miR-128*), and 9 lncRNAs (X-inactive specific transcript [*XIST*]; *ST7-AS2*; *LINC00309*; *LINC00299*; *LINC00261*; *LINC00276*; *LINC00355*; rhabdomyosarcoma 2-associated transcript [*RMST*]; *LINC00520*; and prostate cancer antigen 3 [*PCA3*]; Figure 6). The *XIST-miR-181a-COL4A1* axis was particularly involved in the KC-associated ceRNA regulatory network.

DISCUSSION

Previous studies have suggested that sex and ethnicity may affect morbidity, gene expression, and episode age in KC [20,33,34]. Gender consistency in gene expression, however, will generally explain the pathogenesis of KC. In this study, a total of 282 DE-lncRNAs (192 upregulated and 90 downregulated), 40 DE-miRNAs (29 upregulated and 11 downregulated), and 910 DE-mRNAs (554 upregulated and 356 downregulated) were screened for KC, relative to control samples with no gender bias. For the DE-mRNAs, 13 GO_BP terms, 10 GO_CC terms, 11 GO_MF terms, and 9 KEGG pathways were enriched. In the KC-associated ceRNA regulatory network, there were 6 mRNAs (including *PPARG*, *HLA-B*, *COL4A1*, and *COL4A2*), 5 miRNAs (including *miR-181a*), and 9 lncRNAs (including *XIST*). The number of DE-mRNAs (910) between the KC and control samples was higher than 13 and lower than 1422 without and with gender bias, respectively, in You [20]. The number of DE-mRNAs (910) with strict criteria (edgeR, |log2FC| >1, and FDR <0.05) suggested that the result of the gene expression profile was credible.

The elevated inflammatory factors, including IL-6, TNF-α, and IL-1 receptors, have been identified in KC epithelium, despite KC having been defined as a non-inflammatory condition [8,35-37]. Multiple studies have shown conflicting results about inflammation in KC. Among the reported inflammatory factors in KC, IL-6 and IL-6 receptor (IL-6R) play roles in glaucomatous optic nerve and retina damage, and their abnormal single nucleotide polymorphisms (SNPs) are involved in the development and progression of primary open-angle glaucoma (POAG) [38]. In addition, IL-6 assumes important roles in herpes simplex virus (HSV) type I infection-induced corneal nerve degeneration [39] and in ocular inflammation and angiogenesis in the cornea [40]. The roles of *PPARG* in inflammation have been widely reported [41-43]. *PPARG* regulates the redox balance in macrophages [41]. A previous study explored the functions of *PPARG* agonist rosiglitazone on retinoblastoma cells and found that rosiglitazone plays an antitumor role via the suppression of cell growth, metastasis, and invasion and via the promotion of cell apoptosis [44]. *HLA-A26*, *HLA-B40*, and *HLA-DR9* are frequently found in older Japanese populations and may be related to KC in young people [45]. *HLA-G* contributes to establishing immune tolerance in allograft, which may also help to maintain the immune-privileged status of the cornea [46]. Our present study, however, identified the downregulation of IL-6, *PPARG* and *HLA* in epithelium from patients with KC. We speculated the participation of IL-6, *PPARG* and *HLA* in KC pathogenesis. However, there were conflicting

results between our study and others reporting the elevation of IL-6 in KC epithelium compared with controls [8,35-37].

In addition to conflicting inflammatory conditions in KC, histopathological changes in collagen decomposition or fibrosis are associated with KC induction [47,48]. Transcription factor 8 (*TCF8*) plays a role in about half of posterior polymorphous corneal dystrophy (PPCD) cases, and its target, *COL4A3*, is critical in both Alport syndrome and PPCD [49,50]. Enhancement during collagen decomposition is responsible for the damage of pathological tissues in KC corneas, which is still retained in initial cultures of KC fibroblasts [51]. In KC corneas, type I, III, and V collagens have no difference in distribution, while the distribution of type IV collagen is disruptive and excrescent in the corneal basement membrane [47,52]. KC corneas have decreased collagen protein levels, and collagen type IV functions as a candidate gene in the development of KC [53]. Our present study suggested that *COL4A1* and *COL4A2* were dysregulated in the KC epithelium relative to controls, suggesting the crucial role of collagen decomposition in the progression of KC.

In addition to the DE-mRNAs, we also identified the DE-miRNAs and lncRNAs in KC samples compared with controls. The *miR-181a*, *miR-21*, and Smad signaling coordinately regulate the expression of TGF-β-induced gene (*TGFBI*) protein (TGFBIp) in corneal fibroblasts, and their pharmacologic modulation may be applied to treat *TGFBI*-correlated corneal dystrophy [54]. The overexpression of *miR-181b* can be induced by hypoxia, which further promotes the angiogenesis of retinoblastoma cells by mediating GATA-binding protein 6 (*GATA6*) and programmed cell death 10 (*PDCD10*) [55]. Upregulated lncRNA *XIST* is positively related to an advanced stage and late differentiation state of retinoblastoma, and *XIST* may accelerate retinoblastoma progression via regulating the *miR-124*/signal transducer and activator of transcription 3 (*STAT3*) axis [56]. The *XIST-miR-181a-COL4A1* axis was involved in the KC-associated ceRNA regulatory network, indicating that *XIST* and *miR-181a* might be correlated with the pathogenesis of KC through the *XIST-miR-181a-COL4A1* axis.

In conclusion, 282 DE-lncRNAs, 40 DE-miRNAs, and 910 DE-mRNAs were identified between the KC and control samples. These DE-RNAs were identified without gender bias. Further, *PPARG*, *HLA-B*, *COL4A1*, *COL4A2*, *miR-181a*, and *XIST* might be involved in the development and progression of KC in both females and males. Moreover, the *XIST-miR-181a-COL4A1* axis might function in the mechanisms of KC. However, the specific roles of these RNAs in KC should be further explored and supported by experiments.

REFERENCES

1. Sherwin T, Brookes NH. Morphological changes in keratoconus: pathology or pathogenesis. Clin Experiment Ophthalmol 2004; 32:211-7. [PMID: 15068441].

2. Léoni-Mesplié S, Mortemousque B, Mesplié N, Touboul D, Praud D, Malet F, Colin J. Epidemiological aspects of keratoconus in children. J Fr Ophtalmol 2012; 35:776-85. [PMID: 22981526].

3. Naderan M, Shoar S, Rezagholizadeh F, Zolfaghari M. Characteristics and associations of keratoconus patients. Cont Lens Anterior Eye 2015; 182:199-205. [PMID: 25707930].

4. Lehtosalo J, Uusitalo RJ, Mianowizc J. Epikeratophakia for treatment of keratoconus. Acta Ophthalmol Suppl 1987; 65:S18274-7. [PMID: 2837066].

5. Espandar L, Meyer J. Keratoconus: overview and update on treatment. Middle East Afr J Ophthalmol 2010; 17:15-20. [PMID: 20543932].

6. Grünauer-kloevekorn C, Duncker GI. Keratoconus: epidemiology, risk factors and diagnosis. Klin Monatsbl Augenheilkd 2006; 223:493-502. [PMID: 16804819].

7. Khaled ML, Bykhovskaya Y, Yablonski SE, Li H, Drewry MD, Aboobakar IF, Estes A, Gao X, Stamer WD, Xu H. Differential Expression of Coding and Long Noncoding RNAs in Keratoconus-Affected Corneas. Invest Ophthalmol Vis Sci 2018; 59:2717-28. [PMID: 29860458].

8. Pahuja N, Kumar NR, Shroff R, Shetty R, Nuijts RM, Ghosh A, Sinha-Roy A, Chaurasia SS, Mohan RR. Differential Molecular Expression of Extracellular Matrix and Inflammatory Genes at the Corneal Cone Apex Drives Focal Weakening in Keratoconus. Invest Ophthalmol Vis Sci 2016; 57:5372-82. [PMID: 27732724].

9. Ionescu C, Corbu CG, Tanase C, Jonescu-Cuypers C, Nicula C, Dascalescu D, Cristea M, Voinea LM. Inflammatory Biomarkers Profile as Microenvironmental Expression in Keratoconus. Dis Markers 2016; 2016:1-8. [PMID: 27563164].

10. Shetty R, Anuprita G, Lim RR, Murali S, Krina M, Reshma AR, Ashwini R, Sriharsha N, Nuijts RMMA, Roger B. Elevated expression of matrix metalloproteinase-9 and inflammatory cytokines in keratoconus patients is inhibited by cyclosporine A. Invest Ophthalmol Vis Sci 2015; 56:738-50. [PMID: 25648341].

11. Karolak JA, Polakowski P, Szaflik J, Szaflik JP, Gajecka M. Molecular Screening of Keratoconus Susceptibility Sequence Variants in VSX1, TGFBI, DOCK9, STK24, and IPO5 Genes in Polish Patients and Novel TGFBI Variant Identification. Ophthalmic Paediatr Genet 2016; 37:37-43. [PMID: 24940934].

12. Abu-Amero KK, Helwa I, Almuammar A, Strickland S, Hauser MA, Allingham RR, Liu Y. Screening of the Seed Region of MIR184 in Keratoconus Patients from Saudi Arabia. BioMed Res Int 2015; 2015:604508-[PMID: 26380287].

13. Hughes AE, Bradley DT, Campbell M, Lechner J, Dash DP, Simpson DA, Willoughby CE. Mutation altering the miR-184 seed region causes familial keratoconus with cataract. Am J Hum Genet 2011; 89:628-33. [PMID: 21996275].

14. Li X, Bykhovskaya Y, Tang YG, Picornell Y, Haritunians T, Aldave AJ, Szczotka-Flynn L, Iyengar SK, Rotter JI, Taylor KD. An association between the calpastatin (CAST) gene and keratoconus. Cornea 2013; 32:696-701. [PMID: 23449483].

15. Joseph R, Srivastava OP, Pfister RR. Downregulation of β-actin gene and human antigen R in human keratoconus. Invest Ophthalmol Vis Sci 2012; 53:4032-[PMID: 22562506].

16. Mercer TR, Dinger ME, Mattick JS. Long non-coding RNAs: insights into functions. Nat Rev Genet 2009; 10:155-9. [PMID: 19188922].

17. Wapinski O, Chang HY. Long noncoding RNAs and human disease. Trends Cell Biol 2011; 21:354-61. [PMID: 21550244].

18. Paraskevopoulou MD, Hatzigeorgiou AG. Analyzing MiRNA–LncRNA Interactions. Methods Mol Biol 2016; 1402:271-86. [PMID: 26721498].

19. Ergun S, Oztuzcu S. Oncocers: ceRNA-mediated cross-talk by sponging miRNAs in oncogenic pathways. Tumour Biol 2015; 36:1-8. [PMID: 25809705].

20. You J, Corley SM, Wen L, Hodge C, Höllhumer R, Madigan MC, Wilkins MR, Sutton G. RNA-Seq analysis and comparison of corneal epithelium in keratoconus and myopia patients. Sci Rep 2018; 8:389-[PMID: 29321650].

21. Null RCTR, Team R, Null RCT, Core Writing T, Null R, Team R. Null RDCT, Core R, Team R, Team RDC. R: A language and environment for statistical computing. Computing 2009; 1:12-21. .

22. Povey S, Lovering R, Bruford E, Wright M, Lush M, Wain H. The HUGO Gene Nomenclature Committee (HGNC). Hum Genet 2001; 109:678-80. [PMID: 11810281].

23. Nikolayeva O, Robinson MD. edgeR for differential RNA-seq and ChIP-seq analysis: an application to stem cell biology. Methods Mol Biol 2014; 1150:45-79. [PMID: 24743990].

24. Kolde R. Pretty Heatmaps. R package. 2015. https://cran.r-project.org/web/packages/pheatmap/index.html.

25. Glynn Dennis J, Sherman BT, Hosack DA, Yang J, Gao W, Lane HC, Lempicki RA. DAVID: Database for Annotation, Visualization, and Integrated Discovery. Genome Biol 2003; 4:3-[PMID: 12734009].

26. Young MD, Wakefield MJ, Smyth GK, Oshlack A. Gene ontology analysis for RNA-seq: accounting for selection bias. Genome Biol 2010; 11:R14-.

27. Zhang T, Jiang M, Chen L, Niu B, Cai Y. Prediction of gene phenotypes based on GO and KEGG pathway enrichment scores. BioMed Res Int 2013; xxx:870795-.

28. Yang C, Wu D, Gao L, Liu X, Jin Y, Wang D, Wang T, Li X. Competing endogenous RNA networks in human cancer: hypothesis, validation, and perspectives. Oncotarget 2016; 7:13479-90. [PMID: 26872371].

29. Jeggari A, Marks DS, Larsson E. miRcode: a map of putative microRNA target sites in the long non-coding transcriptome. Bioinformatics 2012; 28:2062-3. [PMID: 22718787].

30. Li JH, Liu S, Zhou H, Qu LH, Yang JH. starBase v2.0: decoding miRNA-ceRNA, miRNA-ncRNA and protein-RNA interaction networks from large-scale CLIP-Seq data. Nucleic Acids Res 2014; 42:D92-[PMID: 24297251].

31. Kohl M, Wiese S, Warscheid B. Cytoscape: software for visualization and analysis of biological networks. Methods Mol Biol 2011; 696:291-303. [PMID: 21063955].

32. Peter DA, Grondin MC, Robin J, Lay JM, Kelley LH, Cynthia SR, Daniela S, King BL, Rosenstein MC, Wiegers TC. The Comparative Toxicogenomics Database: update 2013. Nucleic Acids Res 2013; 41:1104-14. [PMID: 23222133].

33. Magalhaes OA, Marafon SB, Ferreira RC. Gender differences in keratoconus keratoplasty: a 25-year study in Southern Brazil and global perspective. Int Ophthalmol 2018; 38:1627-33. [PMID: 28831627].

34. Suzuki T, Richards SM, Liu S, Jensen RV, Sullivan DA. Influence of sex on gene expression in human corneal epithelial cells. Mol Vis 2009; 15:2554-69. [PMID: 20011627].

35. Krachmer JH, Feder RS, Belin MW. Keratoconus and related noninflammatory corneal thinning disorders. Surv Ophthalmol 1984; 28:293-322. [PMID: 6230745].

36. Galvis V, Sherwin T, Tello A, Merayo J, Barrera R, Acera A. Keratoconus: an inflammatory disorder? Eye (Lond) 2015; 29:843-59. [PMID: 25931166].

37. Rohit S, Anuprita G, Lim RR, Murali S, Krina M, Reshma AR, Ashwini R, Sriharsha N, Nuijts RMMA, Roger B. Elevated expression of matrix metalloproteinase-9 and inflammatory cytokines in keratoconus patients is inhibited by cyclosporine A. Invest Ophthalmol Vis Sci 2015; 56:738-50. [PMID: 25648341].

38. Zhou G, Liu B, Yang YF. Single nucleotide polymorphism analysis of multi-loci and -genes in primary open-angle glaucoma with pathological myopia. Int J Ophthalmol 2007; 3:36-42

39. Chucair-Elliott AJ, Jinkins J, Carr MM, Carr DJJ. IL-6 Contributes to Corneal Nerve Degeneration after Herpes Simplex Virus Type I Infection. Am J Pathol 2016; 186:2665-78. [PMID: 27497323].

40. Ghasemi H. Roles of IL-6 in Ocular Inflammation: A Review. Ocul Immunol Inflamm 2018; 26:37-50. [PMID: 28146368].

41. Shua Y. yang N, Bei Y, Shen P. PPARγ phosphorylation at Ser186 regulates metabolic inflammation via modulating redox balance in adipocyte tissue macrophages. Free Radic Biol Med 2018; 120:s156-.

42. Sardella C, Winkler C, Quignodon L, Hardman JA, Toffoli B, Gmp GA, Hundt JE, Michalik L, Vinson CR, Paus R. Delayed Hair Follicle Morphogenesis and Hair Follicle Dystrophy in a Lipoatrophy Mouse Model of Pparg Total Deletion. J Invest Dermatol 2017; 138:xxx-.

43. Nobs SP, Natali S, Pohlmeier L, Okreglicka K, Schneider C, Kurrer M, Sallusto F, Kopf M. PPARγ in dendritic cells and T cells drives pathogenic type-2 effector responses in lung inflammation. J Exp Med 2017; 214:3015-35. [PMID: 28798029].

44. Cao X, Lin H, Li Y. Effects of PPARγ agonistrosiglitazone on human retinoblastoma cell in vitro and in vivo. Int J Clin Exp Pathol 2015; 8:12549-56. [PMID: 26722443].

45. Adachi W, Mitsuishi Y, Terai K, Nakayama C, Hyakutake Y, Yokoyama J, Mochida C, Kinoshita S. The association of HLA with young-onset keratoconus in Japan. Am J Ophthalmol 2002; 133:557-9. [PMID: 11931792].

46. Le DM, Moreau PP, Legeais JM, Carosella ED. Expression of HLA-G in human cornea, an immune-privileged tissue. Hum Immunol 2003; 64:1039-44. [PMID: 14602233].

47. Kenney MC, Brown DJ. The Cascade Hypothesis of Keratoconus. Cont Lens Anterior Eye 2003; 26:139-46. [PMID: 16303509].

48. Smolek MK, Beekhuis WH. Collagen fibril orientation in the human corneal stroma and its implications in keratoconus. Invest Ophthalmol Vis Sci 1997; 38:1289-[PMID: 9191590].

49. Krafchak Charles M, Pawar H, Moroi Sayoko E, Sugar A, Lichter Paul R, Mackey David A, Mian S, Nairus T, Elner V, Schteingart Miriam T. Mutations in TCF8 Cause Posterior Polymorphous Corneal Dystrophy and Ectopic Expression of COL4A3 by Corneal Endothelial Cells. Am J Hum Genet 2005; 77:694-708. [PMID: 16252232].

50. Kokolakis NS, Maria G, Chatziralli IP, Chryssanthi K, Zisis G, Peponis VG, Droutsas KD, Christos K, Nicholas A, Dimitrios M. Polymorphism analysis of COL4A3 and COL4A4 genes in Greek patients with keratoconus. Ophthalmic Genet 2015; 36:213-7. [PMID: 24099280].

51. Ihalainen A, Salo T, Forsius H, Peltonen L. Increase in type I and type IV collagenolytic activity in primary cultures

of keratoconus cornea. Eur J Clin Invest 2010; 16:78-84. [PMID: 3009200].

52. Nakayasu K, Tanaka M, Konomi H, Hayashi T. Distribution of types I, II, III, IV and V collagen in normal and keratoconus corneas. Ophthalmic Res 2009; 18:1-10. [PMID: 3513078].

53. Saravani R, Hasanian-Langroudi F, Validad MH, Yari D, Bahari G, Faramarzi M, Khateri M, Bahadoram S. Evaluation of Possible Relationship Between COL4A4 Gene Polymorphisms and Risk of Keratoconus. Cornea 2015; 34:318-22. [PMID: 25651396].

54. Choi SI, Jin JY, Maeng YS, Kim TI, Kim EK. TGF-β regulates TGFBIp expression in corneal fibroblasts via miR-21, miR-181a, and Smad signaling. Biochem Biophys Res Commun 2016; 472:150-5. [PMID: 26915797].

55. Xu X, Ge S, Jia R, Zhou Y, Song X, Zhang H, Fan X. Hypoxia-induced miR-181b enhances angiogenesis of retinoblastoma cells by targeting PDCD10 and GATA6. Oncol Rep 2015; 33:2789-96. [PMID: 25872572].

56. Hu C, Liu S, Han M, Wang Y, Xu C. Knockdown of lncRNA XIST inhibits retinoblastoma progression by modulating the miR-124/STAT3 axis. Biomed Pharmacother 2018; 107:547-54. .